



Hybrid-steel concrete connections under reversed cyclic loadings

Bing Li, W.K. Yip and C.L. Leong

Nanyang Technological University, Sch. of Civil & Env. Eng., Singapore 639798

ABSTRACT: The aim of the test was to develop a preliminary guideline for the overall design and construction of precast concrete structures for lateral load resistance. Specimens were tested under reversed cyclic loading to evaluate their ductility, strength and energy dissipation capacity characteristics. Four beam-column joint with slab were tested and the results are presented. MJ1 & MJ2 were monolithic specimens while their precast counterparts CJ1 & CJ2 were constructed using the proposed hybrid-steel concrete connections for a precast concrete frame. Although the structural behaviour was generally similar, different cracking pattern was found. The results indicate that the proposed hybrid-steel concrete connections for precast concrete frame are conceptually sound but and can be refined in design detailing for enhanced performance. It was found that the discontinuity in the bottom reinforcement of the precast beams caused the formation of a lower lever arm, which eventually led to a lower moment capacity of the specimens. The precast specimens however, behaved similarly to their monolithic counterparts and showed consistent hysteresis loops characteristics throughout the test.

1 INTRODUCTION

In Singapore, the use of precast concrete for structural elements in buildings for public sector projects has increased steadily since the 1990s. However, great attention being devoted to the design of individual precast element with little attention given to the connection of each component. The connection detail is not taken into consideration until the finalisation of the structural concept. However, the connection design is one of the most important considerations in the successful application of precast concrete technology to achieve buildability. The design and detailing of the connection for example, influence the strength, stability, ductility and the load redistribution of the structure.

Research on hybrid-steel concrete connections for precast concrete frames has been carried out in Nanyang Technological University, Singapore, since 1997. The pilot studies on the structural behaviour of precast beam and precast column were completed in the initial stage. Crucial parameters such as the embedded length of inserted I-beam have been verified through experimental results. Additionally, six cruciform precast hybrid steel-concrete joints were tested to verify their performance as semi-rigid joints. Sufficient information on the behaviour of hybrid-steel concrete connections in precast concrete frames has been gathered from these past research work. It now seems timely to refine the design principles to verify the ability of these connections to resist lateral loading.

2 TEST PROGRAMME

All specimens were tested under lateral loading using the steel loading frame as shown in Figure 1. At each end of the column, steel plates with pin holes are bolted to the column through bolts that are encased in the concrete. The bottom of the column is connected to the strong floor through a pin joint. A 500kN capacity double acting hydraulic actuator is used to effect the reversed cyclic lateral loads. One end of the actuator is pin-connected to the top of the column, while the other one is pin-connected to the steel loading frame.

moderate seismicity regions is much lower. Normal strength concrete of grade 40 was used in the specimens. On the other hand, the ratio of calculated column-to-beam flexural strength, based on the strain compatibility equilibrium approach, was 1.36 and 0.47 for specimens MJ1 (or CJ1) and MJ2 (or CJ2) respectively. The summary of material used is shown in Table 1.

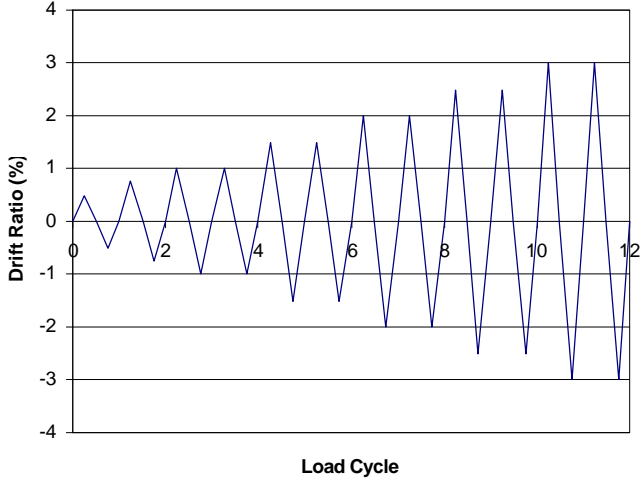


Figure 2: Loading Pattern

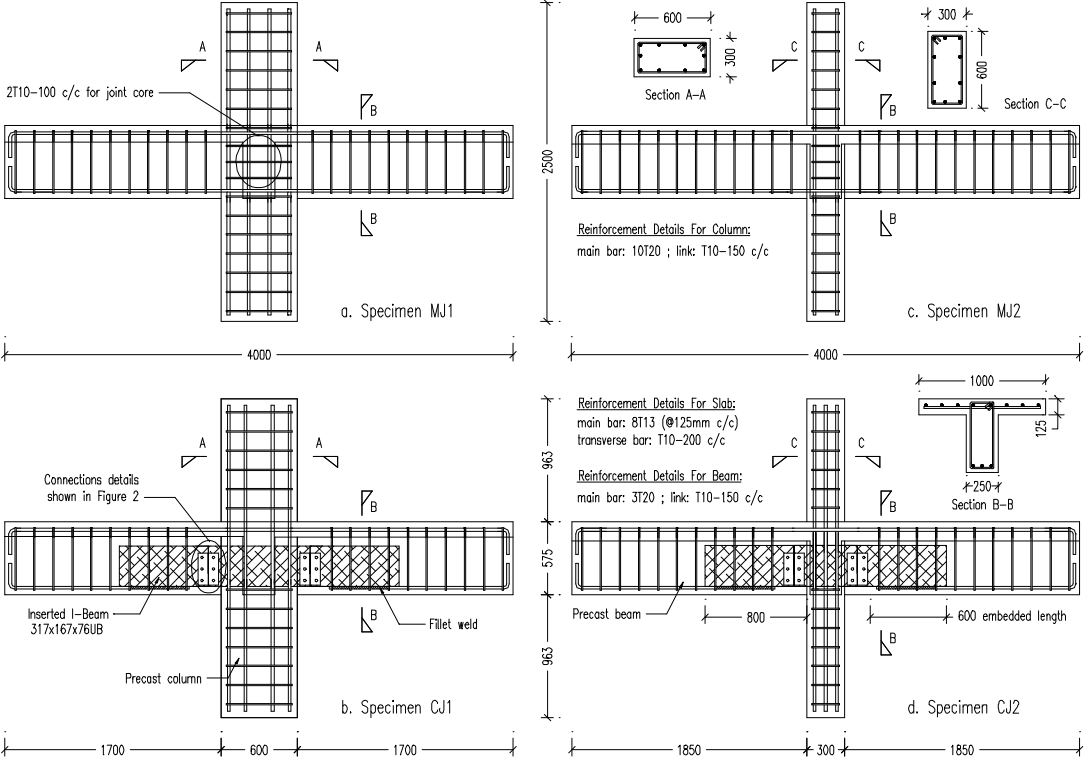


Figure 3: Details of Specimens

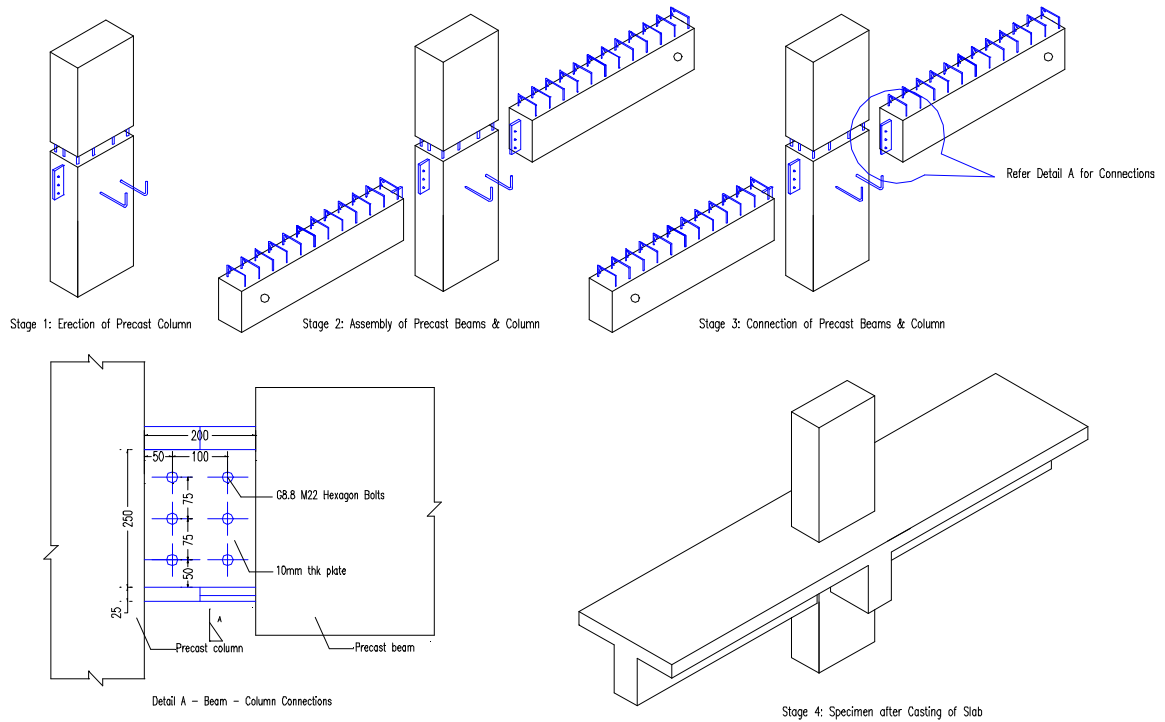


Figure 4: Connection Details of Typical Precast Specimens

Table 1: Summary of material used

Material	Strength (MPa)
Concrete (f_c')	40 (concrete cover 30mm)
R10 Reinforcement	400
T13 Reinforcement	550
T22 Reinforcement	580
317×167×76UB (web)	493
317×167×76UB (flange)	181
254×254×89 UC (web)	531
254×254×89 UC (flange)	217
10mm thick steel plate	327

4 EXPERIMENTAL RESULTS AND DISCUSSIONS

4.1 Overall Response

Both specimens CJ1 and CJ2 exhibited similar structural behaviour as those of the monolithic specimens MJ1 and MJ2 in the initial stage of loading. However, they behaved differently from their monolithic counterparts after cracking had occurred. The monolithic specimens MJ1 and MJ2 generally showed a stable energy dissipation capacity with cracks all over the specimens. These

specimens behaved in a ductile manner. For specimens CJ1 and CJ2, no brittle failure was observed throughout the test but the level of energy dissipation and strength achieved was less than those of their monolithic counterparts regardless of the orientation of the columns. The possibility of the bolt connection failure was ruled out, as there was no sudden or brittle failure. Yielding and local buckling of inserted steel beam or steel plate were not expected as the excess flexibility in the connections caused low stress and was transferred from the columns to beams. Plastic hinges formed at the slab region (beam top) where the reinforcement was found to have yielded. The main cause of the extensive cracking of the slab was due to the yielding of the reinforcement and the concrete crushing under both tension and compression at the beam/slab region.

The specimens with composite connections were designed to fail at the connection. However, due to the built-in tolerance between the bolts and bolt-holes (which was about 2-3mm of the hole diameter), the structure tended to have lower ductility, as the result of the high flexibility in the precast beams at the beam/column connection. It would be ideal if the connection region served as designated plastic hinges but the over-flexibility of the connections caused the slippage to occur instead of the formation of plastic hinges.

Insufficient aggregate interlocking at the cold joints between the precast beams and the infill concrete at the bolted connections was another source of low stiffness in the precast specimens. The discontinuity in the bottom reinforcement of the beams also affected the low stiffness of the specimens. In the sagging moment stage, the bottom of the beam was in tension. Since the aggregate interlocking was lacking, the initial flexural cracks appeared and propagated rapidly with increasing load, forming vertical cracks between the beam and connection region. With the absence of continuity in the bottom reinforcement, the vertical cracks propagated more rapidly, causing the beams to lose their ability to resist the sagging moment.

4.2 Load-Displacement Response (Hysteresis Loops)

The lateral load-displacement hysteresis loops of each specimen are shown in Figures 5a to 5d. Comparison between the precast specimens and their monolithic counterparts are shown to give a clearer picture on the evaluation of their strength, ductility and energy dissipation capacity characteristics.

Figure 5a shows the hysteresis loop of specimen MJ1. This specimen generally showed a satisfactory strength, ductility and energy dissipation characteristic. The stiffness and strength increased as the load was applied from DR 0.5% until DR 2.0% (approximately from 13mm to 55mm in displacement). The stiffness started to decrease as the DR reached 2.5% (68mm in displacement). This was due to the occurrence of severe cracks that did not fully close when the load was reversed. Pinching was also noticed as DR exceeded 2.0% and yielding of the reinforcement took place as shown by the flat plateau in the curve.

The hysteresis loops for specimen CJ1 are shown in Figure 5b. The loops for its monolithic counterpart MJ1 are also included for comparison. It is obvious that the composite specimen CJ1 also shows good characteristics in energy dissipation, as the enclosed areas of the loops are large and stable. However, pinching was very obvious throughout the test when DR exceeded 1.5% (approximately 41mm displacement). This was due to the rapid opening and closing of cracks along the interface between the precast beam and infill concrete at the connection region, when the load was applied and then reversed. The tolerance in the simple shear connections that contributed to the excess flexibility of those specimens also resulted in the pinching of the hysteresis loops. The maximum load was achieved when displacement equivalent to DR 1.5% was applied and yielding of the reinforcement took place.

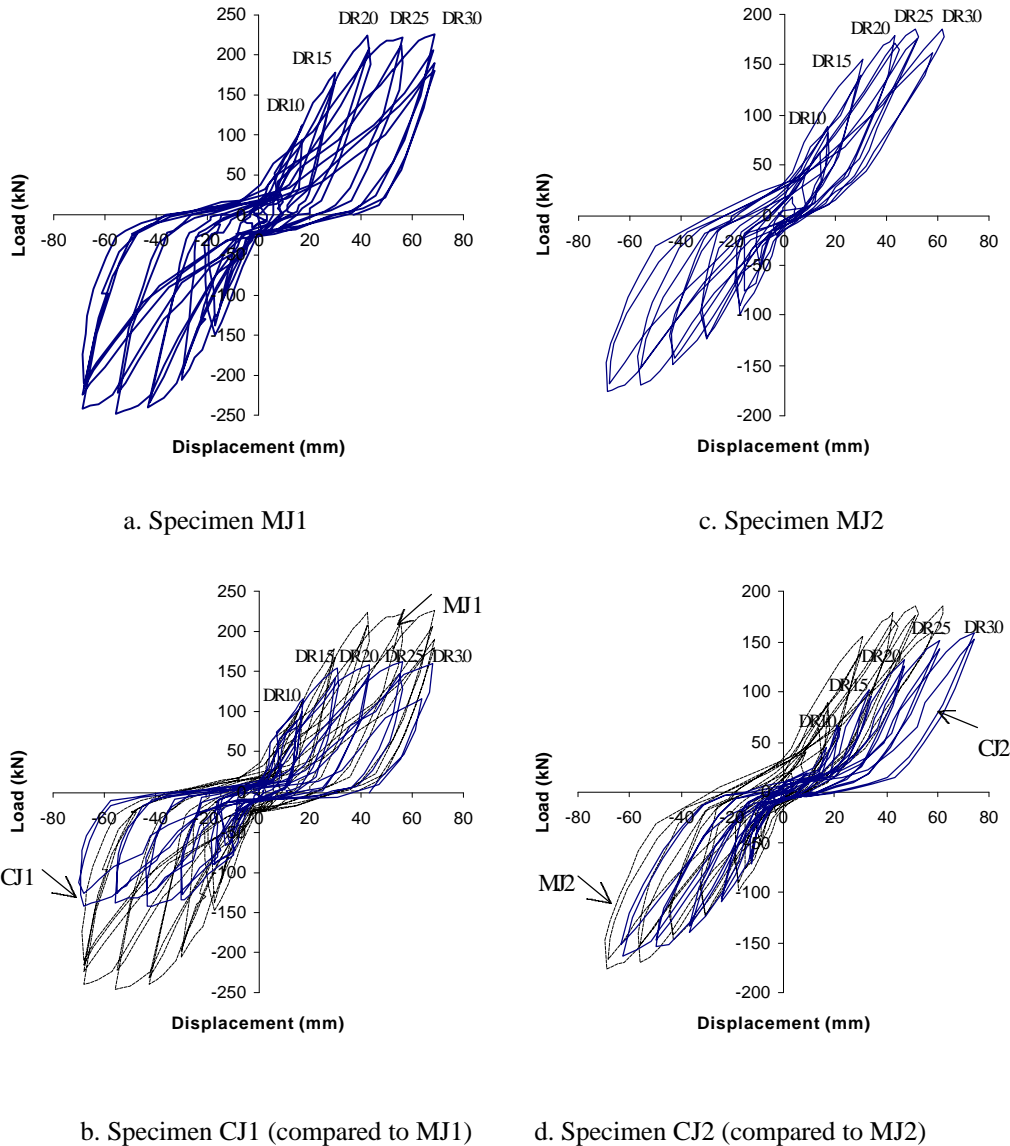


Figure 5: Hysteresis Loops of Specimens

It is noted in Figure 5b that the hysteresis loops in negative region are greater than the loops in the positive regions but with lower maximum attained loads. When the load was first applied to the specimen (the pushing load is designated the negative sign), cracking took place and an attained pushing load was recorded. For the flanged beam section in which there was no continuity of the bottom reinforcing bars in the beam web, the effective lever arm was considered from the bottom bolt of the bolted connection. The value of this lever arm was about 80% of the lever arm of the normal monolithic specimen. This situation caused a lower maximum load to be attained as a lower lever arm was involved. However, when the load was reversed, the beam section reverted to a rectangular section. The position of the lever arm became that of a monolithic beam and hence, a larger load was attained. However, due to the cracking that had occurred in the previous load cycle, some energy had been used to close the cracks and therefore, the loops that formed in the positive region were relatively smaller.

Specimen MJ2 is similar in dimensions to MJ1 except for the orientation of the column direction. Its hysteresis loops are shown in Figures 5c. It is noted that the level of energy dissipation for this specimen is lower than both MJ1 and CJ1 as the specimen has a weaker column stiffness when compare to MJ1. From calculations of flexural strength based on the strain compatibility equilibrium approach, the yielding strength for the column of MJ2 was 104 kN and that for the beams was 205 kN.

The specimen attained a higher strength due mainly to the higher column strength in excess of 85% of its theoretical flexural capacity. This was confirmed by the occurrence of excessive curvature of the column after the test.

Similarly, the energy dissipation of CJ2 was less than that of MJ2, as shown in Figure 5d. This conforms to the characteristics of structures with a ratio of calculated column-to-beam flexural strength less than unity. The strength of the specimen was derived mainly from the higher strength capacity of the column. Pinching was obvious throughout the test and the causes were the same as those for CJ1. The influence of discontinuity in the bottom reinforcement was not too significant in this specimen as the maximum load for CJ2 was close to its monolithic counterpart. The weaker column stiffness was the main cause of failure in CJ2 and MJ2.

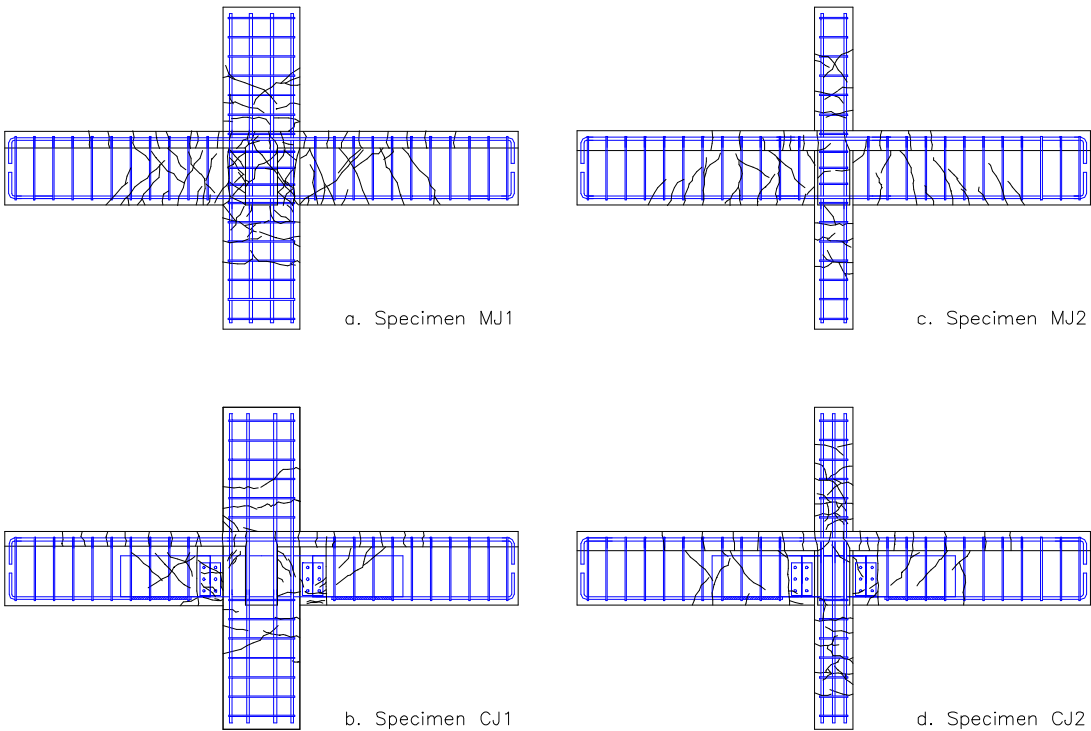


Figure 6: Crack Patterns of Specimens

4.3 Cracking Patterns

The visible cracks of all specimens at the end of the test are shown in Figures 6a to 6d. Generally, extensive cracks formed in the monolithic specimen MJ1 as shown in Figure 6a. These include flexural cracking of the beam due to both the sagging and hogging moments, and diagonal cracks due to shearing at the beam/column junction.

As indicated in Figure 6b, the distinct difference between CJ1 and MJ1 was the formation of vertical cracks that occurred at the interface joint between the composite beam and the concrete infill at the connection region. The discontinuity in the bottom reinforcement caused CJ1 to lose part of its ability to transfer the full beam sagging moment at the column and hence little diagonal cracking caused by the sagging moment was noticed.

Less cracking was found in the beams of MJ2. For MJ2, the column flexural capacity was lower than that of the beam and hence induced a more rapid cracking formation in the column. As shown in Figure 6c, the cracks at the column formed along the column and intersected each other. As shown in Figure 6d, the discontinuity in the bottom reinforcement of the beams and a low column flexural capacity caused closely spaced cracks to form in the column of CJ2. Similar to CJ1, the formation of vertical cracking was found at the interface joint and no diagonal cracking was observed in CJ2.

5 CONCLUSIONS

Based on the test results and observations, the following conclusions can be drawn:

1. All tested specimens showed satisfactory results in their strength, ductility and energy dissipation capacity characteristics.
2. The proposed hybrid connection system in the study is feasible in term of construction technology.
3. The precast specimens however achieved a consistent hysteresis loops throughout the test and behaved similarly to their monolithic counterparts in energy dissipation characteristics.
4. Due to the limitation in the proposed connection, discontinuity in bottom reinforcement was adopted. This condition eventually influenced the effective lever arm of the beams and thus limited the strength development of the precast specimens to match that of their monolithic counterparts.

6 ACKNOWLEDGEMENT:

The research funding for this project by the Nanyang Technological University (NTU) and Building Construction Authority (BCA) is highly acknowledged.

REFERENCES

- British Standards Institutions, 1997. "Structural Use of Concrete BS 8110, Part 1, code of practice for design and construction; 1997". London: BSI.
- Hakuto S., Park R. and Tanaka H., 2000. "Seismic Load Tests on Interior and Exterior Beam-Column Joints with Substandard Reinforcing Details". *ACI Structural Journal*, V 97, No. 1, Jan-Feb 2000. Detroit: ACI.